

This work was written as part of one of the author's official duties as an Employee of the United States Government and is therefore a work of the United States Government. In accordance with 17 U.S.C. 105, no copyright protection is available for such works under U.S. Law.

Public Domain Mark 1.0

<https://creativecommons.org/publicdomain/mark/1.0/>

Access to this work was provided by the University of Maryland, Baltimore County (UMBC) ScholarWorks@UMBC digital repository on the Maryland Shared Open Access (MD-SOAR) platform.

Please provide feedback

Please support the ScholarWorks@UMBC repository by emailing scholarworks-group@umbc.edu and telling us what having access to this work means to you and why it's important to you. Thank you.



Evidence of a Cascade and Dissipation of Solar-Wind Turbulence at the Electron Gyroscale

F. Sahraoui*

*NASA Goddard Space Flight Center, Code 673, Greenbelt, Maryland 20771, USA
and Laboratoire de Physique des Plasmas, CNRS-Ecole Polytechnique, Vélizy, 78140, France*

M. L. Goldstein

NASA Goddard Space Flight Center, Code 673, Greenbelt, Maryland 20771, USA

P. Robert

Laboratoire de Physique des Plasmas, CNRS-Ecole Polytechnique, Vélizy, 78140, France

Yu. V. Khotyaintsev

*Swedish Institute of Space Physics, Uppsala, Sweden
(Received 24 February 2009; published 10 June 2009)*

We report the first direct determination of the dissipation range of magnetofluid turbulence in the solar wind at the electron scales. Combining high resolution magnetic and electric field data of the Cluster spacecraft, we computed the spectrum of turbulence and found two distinct breakpoints in the magnetic spectrum at 0.4 and 35 Hz, which correspond, respectively, to the Doppler-shifted proton and electron gyroscals, f_{ρ_p} and f_{ρ_e} . Below f_{ρ_p} , the spectrum follows a Kolmogorov scaling $f^{-1.62}$, typical of spectra observed at 1 AU. Above f_{ρ_p} , a second inertial range is formed with a scaling $f^{-2.3}$ down to f_{ρ_e} . Above f_{ρ_e} , the spectrum has a steeper power law $\sim f^{-4.1}$ down to the noise level of the instrument. We interpret this as the dissipation range and show a remarkable agreement with theoretical predictions of a quasi-two-dimensional cascade into Kinetic Alfvén Waves (KAW).

DOI: [10.1103/PhysRevLett.102.231102](https://doi.org/10.1103/PhysRevLett.102.231102)

PACS numbers: 96.60.Vg, 52.35.Ra, 94.05.Lk, 95.30.Qd

Observations of solar-wind (SW) turbulence have usually emphasized magnetohydrodynamic (MHD) scales where the Kolmogorov scaling $k^{-5/3}$ is frequently observed [1]. Observations of turbulence at frequencies above the proton gyrofrequency ($f_{cp} \sim 0.1$ Hz) [2,3] and the properties in this range of frequencies and wave numbers have not been thoroughly investigated and remain far less well understood. Above f_{cp} and up to 10 Hz steeper, power law spectra $f^{-\alpha}$ with $2 < \alpha < 4$ have been observed [2–5], and a debate exists as to whether the turbulence has become dispersive following the whistler mode or the KAW branch, before it is dissipated at small scales [6,7]. There are several theoretical predictions concerning small scale turbulence: Biskamp *et al.* [8] predicted a $k^{-7/3}$ magnetic spectrum of whistler turbulence [9,10], and, Galtier [11] derived the $k^{-7/3}$ scaling as an exact solution of the Yaglom's equations for Hall-MHD (HMHD) turbulence. Weak turbulence theory of anisotropic incompressible HMHD predicts a $k_{\perp}^{-5/2}$ scaling for either the whistler or the Alfvén branches [9,11,12]. Gyrokinetic (GK) theory, valid in the strong anisotropy approximation $k_{\parallel} \ll k_{\perp}$ and $\omega \ll \omega_{cp}$, predicts a $k_{\perp}^{-7/3}$ magnetic spectrum [13,14].

In the present Letter, we analyze for the first time very high frequencies (up to 100 Hz) of solar-wind magnetic and electric turbulence by taking advantage of high resolution wave data from the Cluster spacecraft [15]. Magnetic data are from the Flux Gate Magnetometer (FGM) and the STAFF-Search Coil (SC) [16,17] experi-

ments, and electric field data are from the Electric Field and Wave experiment (EFW) [18]. FGM data cover the frequency spectrum up to a few Hz. STAFF-SC and EFW provide higher resolution data with two possible sampling rates: 25 Hz (normal mode) and 450 Hz (burst mode). The data used here are burst mode. Because of the small level of the magnetic turbulence in the SW at these very high frequencies, particular attention has been paid to several instrumental issues, in particular, the sensitivity of the STAFF-SC magnetometer. Because of the low sensitivity of the SC sensor at very low frequency, the lowest part of the STAFF-SC spectra has to be filtered. The cutoff frequency can be set to 0.35 Hz on the two perpendicular components to the spin axis. However, in this study, we filtered the spectra at 1.5 Hz to avoid any residual spin effect.

The data used here were recorded on 19 March 2006 from 20h30 to 23h20 UT in the solar wind at 1 AU. During this period, the Interplanetary Magnetic Field (IMF) was $B \sim 6$ nT, the plasma density $n_p \sim 3$ cm $^{-3}$, the proton and electron temperatures $T_p \sim 50$ eV and $T_e \sim 12$ eV, respectively, the plasma betas (ratios between thermal and magnetic pressures) $\beta_p \sim 2.5$ and $\beta_e \sim 0.7$, respectively, for protons and electrons, the plasma velocity $v \sim 640$ km/s, the Alfvén speed $V_A \sim 65$ km/s, and the proton gyrofrequency $f_{cp} \sim 0.1$ Hz. The plasma data (protons and electrons) have been obtained from the CIS and the PEACE experiments [15].

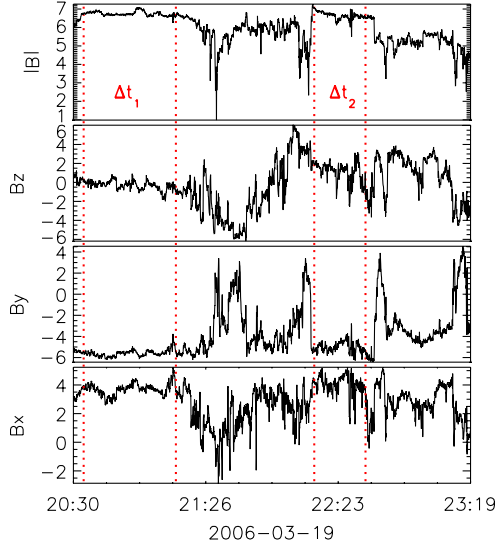


FIG. 1 (color online). FGM magnetic field data measured by Cluster 2 in the solar wind plotted in the Geocentric Solar Ecliptic (GSE) reference frame. The vertical dotted lines delimit two subintervals of time discussed in the text.

Figure 1 shows the magnetic field components measured by FGM. Note the rotations of B_y coincident with a minimum in the magnetic field magnitude, indicating possible multiple current sheet crossings as the spacecraft move from quiet solar wind (Δt_1 in Fig. 1) toward the bow shock. Figure 2 shows the power spectra of the magnetic field data from FGM and STAFF-SC, decomposed into the parallel and the perpendicular directions with respect to the mean IMF (defined by averaging over the time interval of Fig. 1, see [19] and the references therein). These spectra are calculated using a windowed Fourier transform, where a \cos^3 window (having 10% width of the whole interval) is slid to span the time series containing 4×10^6 samples. The spectra shown are the result of averaging all the windows.

Figure 2 illustrates the good matching between the STAFF-SC and the FGM spectra at frequencies around 1.5 Hz. However, above $f \geq 2.5$ Hz, the power in the physical signal falls below the noise floor of the instrument, so we use STAFF-SC data to analyze frequencies above $f \geq 2.5$ Hz. Here, we merge the low frequency FGM data with the STAFF-SC data at $f = 1.5$ Hz. Figure 2 shows a spectral breakpoint at $f \sim 0.4$ Hz where the scaling changes from a Kolmogorov spectrum $f^{-1.62}$ to $f^{-2.5}$. Similar breakpoints and steep spectra have been reported previously [2–5], but mostly attributed to energy dissipation [2,4].

Figure 2 shows, for the first time, clear evidence that the magnetic energy continues cascading for about two decades higher in spacecraft frequency and smaller spatial scales. Furthermore, it shows the first evidence of a second breakpoint at $f \sim 35$ Hz, followed by a steeper spectrum of $f^{-3.9}$. To understand the origin of these breakpoints, we

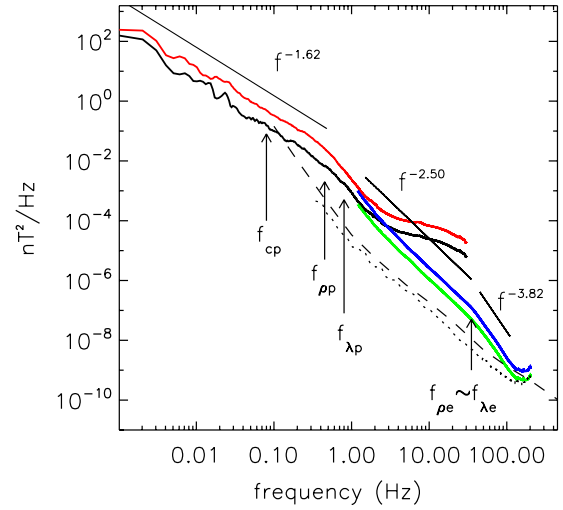


FIG. 2 (color online). The parallel (black) and perpendicular (red) magnetic spectra of FGM data ($f < 33$ Hz) and STAFF-SC data (respectively, light line; green online and dark line; blue online); $1.5 < f < 225$ Hz). The STAFF-SC noise level as measured in the laboratory and in-flight are plotted as dashed and dotted lines, respectively. The straight black lines are power law fits to the spectra. The arrows indicate characteristic frequencies defined in the text.

calculated the characteristic scales of the plasma, namely, the proton and electron gyroscs and inertial lengths defined as $\rho_{p,e} = V_{th,p,e}/\omega_{cp,e}$, $\lambda_{p,e} = V_{A,p,e}/\omega_{cp,e}$, where V_{th} and V_A are the thermal and the Alfvén velocities, and $\omega_{cp,e}$ are the proton and electron gyrofrequencies. Using the Taylor frozen-in-flow hypothesis ($\omega \sim kv$), these scales are Doppler-shifted and represented in Fig. 2. The Doppler-shifted proton and electron gyroscs fit better with the observed breakpoints than do the proton and electron gyrofrequencies (as has been suggested [2,3]). In particular, the ratio of the two frequencies $35/0.4 \sim 90$ is very close to the ratio $\rho_p/\rho_e = \sqrt{m_p T_p/m_e T_e} \sim 95$.

The new breakpoint occurs at the electron gyroscale ρ_e , which is very close to λ_e (because $\beta_e \sim 1$). This can be seen clearly on Fig. 3, which shows the high frequency part of two spectra calculated from the subintervals Δt_1 and Δt_2 of Fig. 1 which have different levels of turbulence. Both spectra show similar properties to those of Fig. 2. The slight difference in the scaling, $f^{-2.5}$ and $f^{-2.3}$, is likely to be due to the discontinuities observed on Fig. 1 and were included in computing the spectra of Fig. 2.

To investigate the nature of the small scale turbulence (i.e., above f_{ρ_p}), we computed the spectrum of the electric field component E_y (shown in Fig. 4). Below f_{ρ_p} the spectrum of E_y shows a high correlation with the spectrum of B_z , and both follow a Kolmogorov scaling. For frequencies around f_{ρ_p} , the E_y spectrum steepens slightly up to $f \sim 1.5$ Hz, where it becomes essentially flat. A fit of the spectrum in the interval $f \sim [1.5, 15]$ Hz shows a power

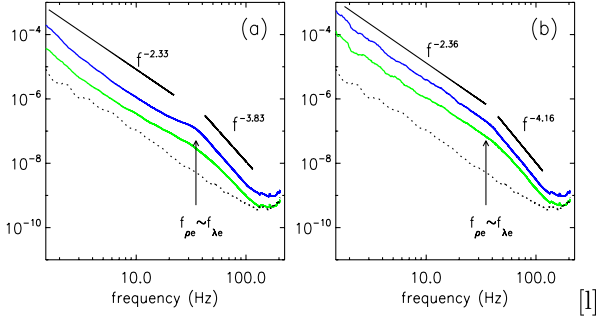


FIG. 3 (color online). High-pass filtered power spectra of the parallel (green line) and perpendicular (blue line) of the magnetic fluctuations measured by STAFF-SC during the time sub-intervals Δt_1 (a) and Δt_2 (b) shown on Fig. 1. Dotted line is the STAFF-SC noise level. The straight black lines are direct power law fits of the spectra. Vertical arrows are defined in the text.

law $\sim f^{-0.3}$. It is worth recalling here that GK theories predict the power laws $k_{\perp}^{-7/3}$ for the magnetic field spectrum and $k_{\perp}^{-1/3}$ for the electric field spectrum at these subproton gyro-scales [13,14]. The fact that the electric field spectrum continues with a nearly zero spectral slope above $f \geq 10$ Hz is due to reaching the noise level of the EFW experiment.

The present observations suggest that the energy of the turbulence is only slightly damped at the proton gyro-scale ρ_p and undergoes another dispersive cascade with the scaling $f^{-2.3}$. Any strong damping would have led to a much steeper spectrum, if not to a clear cutoff [6]. Steepening of spectra (e.g., from $k^{-5/3}$ to $k^{-7/3}$) below the proton scale can indeed be explained solely by dispersive effects as has been predicted by various nondissipative

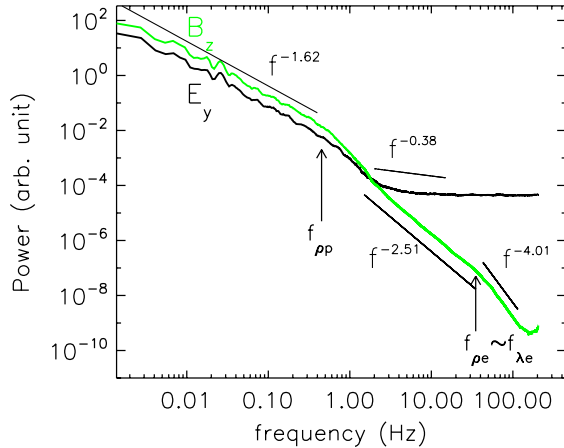


FIG. 4 (color online). Spectra of data from spacecraft 4 in the Despun System of reference (DS): E_y measured by EFW (bold black curve) and B_z measured by FGM and STAFF-SC merged at 1.5 Hz (light line; green online). The straight black lines are direct power law fits of the spectra. Vertical arrows are the Doppler-shifted proton and electron gyro-radius and inertial lengths.

dispersive MHD models [8,9,20,21]. However, as we show below, finite dissipation may occur at the proton scale ρ_p along with more significant damping at the electron gyro-scale ρ_e . This latter may explain the stronger steepening of the spectrum to f^{-4} (the power law fits in the dissipation range may be not very accurate because they extended over less than a decade due to the noise level of the instrument).

This scenario of dispersive cascade and dissipation at electron scales appears consistent with Kinetic Alfvén Wave (KAW) turbulence as predicted by the GK theory [13,14]. The predicted scalings $B^2 \sim k_{\perp}^{-7/3}$ and $E^2 \sim k_{\perp}^{-1/3}$ are in striking agreement with these observations. KAW turbulence has been observed previously [7,22], but only at large (proton) scales (up to 10 Hz). Here, we are observing KAW behavior down to electron scales where enhanced dissipation becomes evident. This can be explained by electron Landau damping, as it is shown below.

To confirm this scenario of KAW energy cascade and dissipation, we have solved numerically the Maxwell-Vlasov equations [23] assuming Maxwellian distributions of protons and electrons with characteristics that reflect the physical parameters deduced from the data. We assumed that the turbulence was quasi-two-dimensional (2D), i.e., $k_{\parallel} \ll k_{\perp}$. This assumption is justified by an analysis (not shown here) that used the k -filtering technique [19] on the \mathbf{k} -vectors distribution at large scales ($f < 10^{-2}$ Hz). That analysis confirmed the 2D nature at large scales. This 2D picture at large scales is likely to continue at the small scales as reported in previous studies [19,22]. Several previous observations have also reported the dominance of the 2D turbulence in the SW [21,24].

The results shown in Fig. 5 prove that under the plasma conditions observed here, KAW can propagate over a wide range of scales before being damped at the electron gyro-

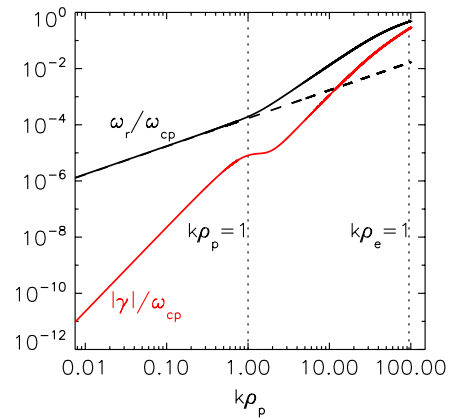


FIG. 5 (color online). Linear solutions of the Maxwell-Vlasov equations for $\theta = \arccos(\mathbf{k}, \mathbf{B}_0) = 89.99^\circ$, obtained using the plasma parameters given in the text. The real part of the frequency (black line) and the damping rate (light line; red online) are consistent with the kinetic Alfvén wave dispersion relation and damping [6,13]. The dashed line is the asymptote $\omega/\omega_{cp} = k_{\parallel}V_A/\omega_{cp}$. The plots stop at scales where $|\gamma| \sim \omega_r$.

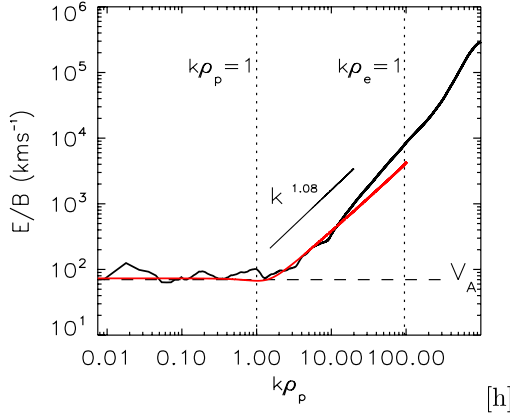


FIG. 6 (color online). The ratio E_y/B_z measured by Cluster 4 (black line) compared to a similar ratio calculated from the linear Maxwell-Vlasov theory (light line; red online). The electric field data have been transformed into the plasma reference frame using the Lorentz transform $\mathbf{E}_{\text{plas}} = \mathbf{E}_{\text{sat}} - \mathbf{V} \times \mathbf{B}$ [7]. The horizontal dashed line is the Alfvén speed. The straight black line is a direct fit of E_y/B_z from $k\rho_p = 1.5$ to $k\rho_p = 20$. We used $\theta = \arccos(\mathbf{k}, \mathbf{v}) = 50^\circ$ to transform frequency to $k\rho_p$.

scale [6,10]. The mode is shown to be only slightly damped at $k\rho_p \sim 1$ where $|\gamma|/\omega_r \sim 0.1$ (γ is the damping rate and ω_r is the real part of the frequency). The KAW mode is however strongly damped by electron Landau resonance at $k\rho_e \sim 1$ where $|\gamma|/\omega_r \sim 1$, which may explain the steepening of the magnetic spectrum to f^{-4} (here, the resonance condition $\omega_r \sim k_{\parallel}V_{\text{th}_e}$ and the KAW dispersion relation $\omega_r = \pm k_{\parallel}V_A k_{\perp} \rho_p / \sqrt{\beta_p + 2/(1 + T_e/T_p)}$ [14] yield the dissipation scale $k\rho_e \sim 0.8$). We notice however that for moderate oblique propagation angles $\leq 80^\circ$, scales $k\rho_p > 15$ are damped by proton Landau or cyclotron resonance ($\omega_r \sim \omega_{\text{cp}}$), which may yield proton heating.

Figure 6 shows a comparison between the ratio of the electric to the magnetic field measured by Cluster and calculated from the linear kinetic theory of the KAW. There is very good agreement between theory and observations: (i) At large scales ($k\rho_p \leq 1$) the similar scaling $E^2 \sim B^2 \sim k^{-1.62}$ yields a constant ratio $V_\phi = E/B \sim V_A$, in agreement with the frozen-in flow approximation $\mathbf{E} = -\mathbf{V} \times \mathbf{B}$; (ii) At the scale $k\rho_p \geq 1$, dispersive effects set in yielding the linear scaling of the phase speed $V_\phi \sim k^{1.08}$, which also agrees with GK theory because $E^2/B^2 \sim k_{\perp}^2 \Rightarrow V_\phi \sim k_{\perp}$. We notice, however, that the linear approximation also predicts that $v_{\phi\parallel}$ is linear in k (from the dispersion relation given above $v_{\phi\parallel} = \omega_r/k_{\parallel} \sim k_{\perp}$). The departure from this linear scaling observed in Fig. 6 for $k\rho_p > 20$ is

due to the noise in the electric field data that causes the flat E_y spectrum mentioned above. One would expect to observe a steepening of the E_y spectrum similar to B_z when the dissipation scale $k\rho_e \sim 1$ is reached [14].

Conclusions.—We have reported the first clear evidence of the cascade of the SW turbulence below the proton gyroscale and its dissipation at the electron gyroscale. We have shown that the kinetic theory of the highly oblique KAW turbulence can account for the observed cascade and dissipation. We found that collisionless electron Landau damping consistently explains the observations rather than proton cyclotron damping. This mechanism of cascade and dissipation at small scales may be applicable in other astrophysical contexts [5,13]. For example, in the solar corona, electron Landau damping, as observed here, may be an efficient mechanism for heating electrons.

The FGM, PEACE, and CIS data come from the CAA (ESA) and AMDA (CESR, France). F. Sahraoui is funded partly by the NPP program at NASA/GSFC.

*Laboratoire de Physique des Plasmas, Vélizy, France; foud.sahraoui@nasa.gov

- [1] W. H. Matthaeus and M. L. Goldstein, *J. Geophys. Res.* **87**, 6011 (1982).
- [2] R. J. Leamon *et al.*, *J. Geophys. Res.* **103**, 4775 (1998).
- [3] O. Alexandrova *et al.*, *Astrophys. J.* **674**, 1153 (2008).
- [4] M. L. Goldstein *et al.*, *J. Geophys. Res.* **99**, 11519 (1994).
- [5] R. J. Leamon *et al.*, *Astrophys. J.* **537**, 1054 (2000).
- [6] O. Stawicki *et al.*, *J. Geophys. Res.* **106**, 8273 (2001).
- [7] S. D. Bale *et al.*, *Phys. Rev. Lett.* **94**, 215002 (2005).
- [8] D. Biskamp *et al.*, *Phys. Plasmas* **6**, 751 (1999).
- [9] V. Krishan and S. M. Mahajan, *J. Geophys. Res.* **109**, A11105 (2004).
- [10] S. P. Gary *et al.*, *Geophys. Res. Lett.* **35**, L02104 (2008).
- [11] S. Galtier, *J. Plasmas Physics* **72**, 721 (2006).
- [12] F. Sahraoui *et al.*, *J. Plasmas Physics* **73**, 723 (2007).
- [13] A. Schekochihin *et al.*, *Astrophys. J.* **182**, 310 (2009).
- [14] G. G. Howes *et al.*, *Phys. Rev. Lett.* **100**, 065004 (2008).
- [15] C. P. Escoubet *et al.*, *The Cluster and Phoenix Missions* (Kluwer Academic Publishers, Belgium, 1995).
- [16] A. Balogh *et al.*, *Ann. Geophys.* **19**, 1207 (2001).
- [17] N. Cornilleau *et al.*, *Ann. Geophys.* **21**, 437 (2003).
- [18] G. Gustafsson *et al.*, *Ann. Geophys.* **19**, 1219 (2001).
- [19] F. Sahraoui *et al.*, *Phys. Rev. Lett.* **96**, 075002 (2006).
- [20] S. Galtier, *Phys. Rev. E* **77**, 015302 (2008).
- [21] W. Matthaeus *et al.*, *J. Geophys. Res.* **95**, 20673 (1990).
- [22] B. Grison *et al.*, *Ann. Geophys.* **23**, 3699 (2005).
- [23] K. Ronmark, *Report 179 of Kiruna Geophys. Inst.* (Kiruna Geophysical Institute, Sweden, 1982).
- [24] T. Osman and T. Horbury, *Astrophys. J.* **654**, L103 (2007).